Chemical Communications

RSCPublishing

COMMUNICATION

DNA adsorption by magnetic iron oxide nanoparticles and its application for arsenate detection

Cite this: DOI: 10.1039/x0xx00000x

Biwu Liu,[a] and Juewen Liu[a]*

Received 00th January 2012,
Accepted 00th January 2012

DOI: 10.1039/x0xx00000x

www.rsc.org/

Iron oxide nanoparticles adsorb fluorescently labeled DNA oligonucleotides via the backbone phosphate and quench fluorescence. Arsenate displaces adsorbed DNA to increase fluorescence, allowing detection of arsenate down to 300 nM. This is a new way of using DNA: analyte recognition relies on its phosphate instead of the bases.

Inorganic arsenic species are extremely toxic; exposure to arsenic has serious adverse health effects,[1-3] damaging skin, heart, liver and kidney and even leading to cancer and death.[4] To manage the arsenic poisoning problem, detection is crucial. The most common arsenic species in water include arsenate (As(V), AsO_4^{3-}) and arsenite (As(III), AsO_3^{3-}).[5] Under oxidizing conditions, arsenate is the dominating form and its protonation state is a strong function of pH. At neutral pH, $H_2AsO_4^-$ and $HAsO_4^{2-}$ co-exist.[6] The detection task is mainly carried out using analytical instruments such as atomic emission[7] or absorption spectroscopy,[8] ICP-MS,[9] or surface enhanced Raman scattering.[10,11] Developing cost-effective biosensors might provide a complementary solution.[12] For example, genetically engineered bacterial cells,[13] and enzyme inhibition assays were developed to detect arsenic.[14,15] On the chemical sensor side, a few optical and electrochemistry assays were reported.[16-19] The World Health Organization (WHO) initially sets a guideline for arsenic in drinking water at 50 μg/L (0.67 μM). In 2001 this was adjusted to 10 μg/L (0.13 μM).

Since phosphate shares similar solution chemistry with arsenate and the free phosphate concentration in potable is very low (<1 μM),[20] we may design sensors based on this. For example, DNA is a polyphosphate and it may be adsorbed by iron oxide. Then arsenate can displace the adsorbed DNA. Given the vast amount of knowledge on DNA detection,[21-25] high sensitivity might be achieved. In this paper, we report DNA-functionalized iron oxide nanoparticle for arsenate detection. Removal of arsenate by iron oxide has been studied for decades. This method works in natural water samples, implying high affinity and selectivity for arsenic. Many studies have compared the adsorption of various anions to iron oxide surface and arsenate binds the strongest.[26-30] A scheme of arsenate adsorption onto iron oxide is presented in Figure 1A, which has been well-characterized by various spectroscopic methods.[26,27]

Given the similarity between phosphate and arsenate, we reason that DNA may also adsorb in a comparable way (Figure 1B). Based on this assumption, we propose a scheme of sensor design (Figure 1C). Using a fluorescently labeled DNA, adsorption onto iron oxide results in fluorescence quenching; arsenate competition then releases the DNA and restores fluorescence signal.

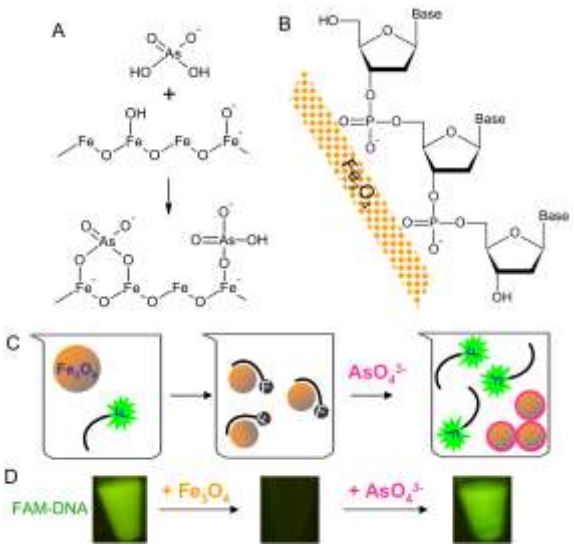

Figure 1. (A) Adsorption of arsenate by iron oxide. (B) Adsorption of DNA by iron oxide by its phosphate backbone. (C) Schematics of sensing arsenate by DNA-functionalized iron oxide NPs. DNA fluorescence is quenched upon adsorption. (D) Fluorescence photographs demonstrating the sensing scheme in (C) using a FAM-labeled 24-mer DNA (500 nM DNA in 25 mM HEPES, pH 7.6). Fe_3O_4 = 10 mg/mL; final arsenate concentration = 40 mM.

To test this hypothesis, we employed Fe_3O_4 NPs with an average size of ~20 nm (see Figure S1 for TEM). These NPs carry a negative charge at neutral pH (ζ-potential = -10 mV in 10 mM HEPES buffer, pH 7.6). Mixing Fe_3O_4 with a FAM-labeled DNA indeed resulted in strong fluorescence quenching (Figure 1D), indicating that DNA can

be adsorbed and Fe_3O_4 is a fluorescence quencher. Addition of arsenate produced strong fluorescence, supporting the mechanism shown in Figure 1C. In the subsequent work, we aim to optimize the DNA adsorption conditions and study sensor performance.

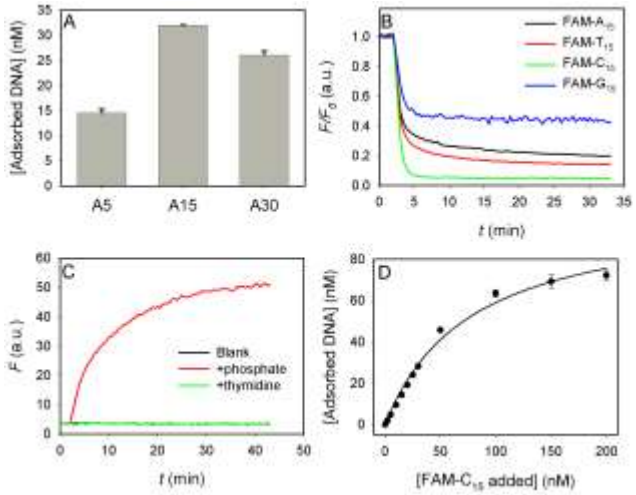

Figure 2. (A) Adsorption capacity of FAM-labeled poly-A DNA as a function of DNA length. The NP concentration was 25 μg/mL and the initial DNA concentration was 50 nM. The buffer contains 10 mM HEPES, pH 7.6 with 300 mM NaCl. (B) Adsorption of FAM-labeled 15-mer DNA with difference sequences. (C) Desorption of the FAM-T_{15} from Fe_3O_4 NPs by free phosphate (1 mM) or thymidine (1 mM), demonstrating DNA adsorption occurs via the phosphate backbone. (D) Adsorption isotherm of FAM-C_{15} DNA.

We first optimized salt concentration. Fluorescence quenching provides a convenient assay to study DNA adsorption. In addition to iron oxide, many other nanomaterials also quench fluorescently labeled DNA.[31-34] Since both DNA and Fe_3O_4 NPs are negatively charged, no DNA was adsorbed in the absence of salt due to strong charge repulsion (Figure S2). Fast adsorption was achieved at higher ionic strength. We chose to perform DNA adsorption with 300 mM NaCl to achieve high adsorption efficiency. Next we varied DNA length (Figure 2A). Considering the scheme in Figure 1C, an ideal sensor should use shorter DNA to achieve a high probe density. The probe needs to cover the NP surface as much as possible, so that arsenate can directly compete with DNA binding instead of occupying free surface sites. However, FAM-A_5 adsorbed much less than FAM-A_{15}, which is attributed to the weaker affinity of shorter DNA. In other words, longer DNA is needed to achieve stable multivalent interactions. FAM-A_{30} also adsorbed less, which is attributed to its larger size and thus occupying more footprint. Therefore, the 15-mer DNA has an optimal length.

Using 15-mer DNA, the effect of DNA sequence was studied (Figure 2B). We assumed that adsorption takes place via the phosphate backbone, and therefore DNA sequence should play a minor role. Indeed, all the four types of homopolymers can be adsorbed. FAM-C_{15} adsorbed with the fastest rate, giving also the lowest background. However, only ~60% FAM-G_{15} was adsorbed. This may be caused by the formation of a G-quadruplex structure, impeding adsorption. To further confirm the adsorption mechanism, a displacement reaction was performed. FAM-T_{15} was first adsorbed and the sample was treated with free phosphate or thymidine (Figure 2C). Strong fluorescence enhancement was observed only with phosphate. Therefore, the base is unlikely to be important for DNA adsorption by iron oxide.

DNA adsorption isotherm was next measured using FAM-C_{15} (Figure 2D). When the added DNA was below 30 nM (Fe_3O_4 concentration = 25 μg /mL), adsorption was quantitative. Further increase of DNA concentration resulted in an overall Langmuir type of isotherm, which is reasonable since adsorption should stop at a monolayer of DNA and adsorption is reversible based on the above phosphate displacement assay. The final capacity is 105 nM DNA, corresponding to 55 FAM-C_{15} molecules on each 20 nm Fe_3O_4 NP. This capacity is lower than adsorption of thiolated DNA by gold NPs, where each 20 nm NP can adsorb ~200 DNA.[35] This lower capacity also indicates that DNA wraps around Fe_3O_4 NPs instead of adopting an upright conformation as in the AuNP system.

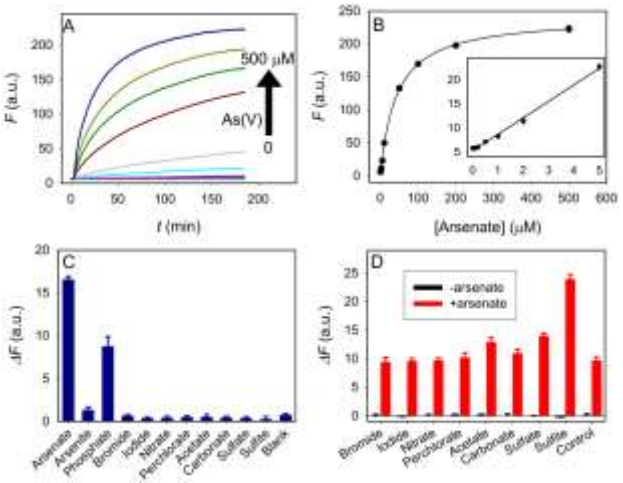

Figure 3. Performance of FAM-C_{15}/Fe_3O_4 conjugates as a sensor for arsenate. (A) Kinetics of sensor fluorescence increase with increasing of arsenate concentration. (B) Sensitivity of arsenate detection. Inset: The initial linear portion. (C) Selectivity against 10 μM other anions. The buffer contained 300 mM NaCl, 10 mM HEPES, pH 7.6. (D) Response of the sensor to 1 mM other anions with or without 10 μM arsenate.

After optimizing DNA adsorption by Fe_3O_4 NPs, we next studied sensor performance using FAM-C_{15} as the probe (Figure 3A). Without arsenate, the sensor has a consistent and low signal, indicating the probe was stably adsorbed. In the presence of arsenate, the sensor fluorescence gradually increased. The kinetics was initially fast followed by a slower phase. A large signal was achieved in just 10 min. Higher concentration of arsenate produced stronger fluorescence enhancement, and the signal increase reached ~35-fold with 500 μM arsenate. The dynamic range goes up to 100 μM arsenate (Figure 3B) and the detection limit was determined to be 300 nM based on the signal higher than three times of background variation (inset of Figure 3B). Another method to further improve sensitivity will be discussed next. To test selectivity, we incubated the sensor with various anions (10 μM) and only phosphate showed a high response (Figure 3C). This is expected since phosphate can also bind to the surface. Systematic comparison of phosphate and arsenate adsorption by iron oxide was previously reported, with arsenate adsorbing slightly more strongly.[29] Since the buffer already contained 300 mM NaCl, we did not test the further addition of chloride. Other anions such as bromide, iodide, nitrate, perchlorate, acetate, bicarbonate, sulphate and sulphite did not produce much

signal. It is interesting to note that arsenite also showed relatively low response, which is consistent with its lower affinity.[36,37] Therefore, this sensor is the most selective for arsenate.

Since phosphate is a limiting nutrient for organism growth and it can be easily precipitated by many cations, its concentration in water is very low (e.g. 1 μM being the upper limit in normal potable water).[20] For other water samples with higher phosphate concentrations, a pre-treatment to precipitate phosphate or a separate phosphate sensor will be needed. We next tested a higher concentration of other anions (1 mM each) and still none of them showed much response (Figure 3D). When 10 μM arsenate was added to these samples, a high response was observed. Sulfite showed even higher response, which might be related to its weak blocking effect to allow arsenate specifically displacing DNA instead of binding to the free iron oxide surface.[28]

An alternative method of detection is to incubate iron oxide NPs with the water sample first, so that adsorption of arsenate might inhibit DNA adsorption for detection (Figure 4A). This method also allows higher sensitivity since a large volume of water sample can be used. Indeed, the detection limit was improved to 50 nM arsenate (Figure 4B). The fluorescence spectra of the samples are shown in Figure S3. This sensitivity is comparable with many other arsenic sensors (Table S1) but it is simpler and cost-effective. Many iron oxide nanoparticles share similar surface properties. In this study, we used Fe_3O_4 and similar observations were also made with Fe_2O_3 NPs (Figure S4).

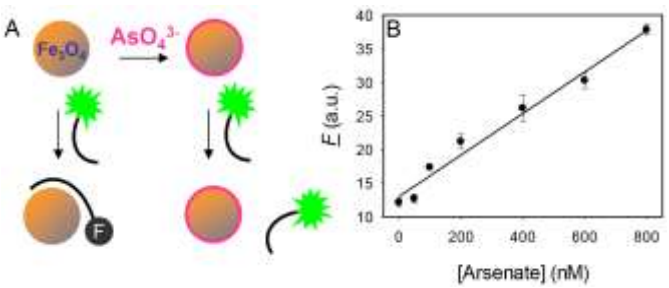

Figure 4. (A) A scheme of detecting arsenate by adsorbing it first before adding probe DNA. (B) Sensitivity of arsenate detection by this arsenate pre-adsorption method.

In summary, we studied DNA adsorption by iron oxide and demonstrated its application for detecting arsenate from water. DNA has been widely used to develop biosensors in the past two decades.[21] In particular, many metal ions are detected using aptamers and DNAzymes, where the DNA bases play a crucial role for metal recognition. Since DNA is a polyanion, DNA has not been very successful in detecting anions, possibly due to charge repulsion. Although arsenate aptamers have been reported,[38] and a few related sensors have been developed,[39] the binding mechanism has not been elucidated. This work provides a new direction for anion sensing using DNA. DNA adsorption by nanomaterials is a popular way of signaling. Compared to previously reported DNA adsorption, the mechanism here is quite different. Binding of DNA to iron oxide is through the phosphate group, which is different from binding to gold (chemisorption through base nitrogen) or carbon (pi-pi stacking and hydrophobic force).[40] Despite this simple interaction, the sensitivity and specificity of the sensor is quite remarkable. This is attributed to the strong affinity between arsenate and iron oxide.

Notes and references

[a] *Department of Chemistry, Waterloo Institute for Nanotechnology, University of Waterloo, Waterloo, Ontario, N2L 3G1, Canada. Fax: 519 7460435; Tel: 519 8884567 Ext. 38919; E-mail: liujw@uwaterloo.ca.*

Electronic Supplementary Information (ESI) available: [methods, TEM and adsorption kinetics]. See DOI: 10.1039/c000000x/

1. B. K. Mandal and K. T. Suzuki, *Talanta*, 2002, **58**, 201-235.
2. D. K. Nordstrom, *Science*, 2002, **296**, 2143-2145.
3. C. F. McGuigan, C. L. A. Hamula, S. Huang, S. Gabos and X. C. Le, *Environ. Rev.*, 2010, **18**, 291-307.
4. W. H. Miller, H. M. Schipper, J. S. Lee, J. Singer and S. Waxman, *Cancer Res.*, 2002, **62**, 3893-3903.
5. X. C. Le, X. F. Lu and X. F. Li, *Anal. Chem.*, 2004, **76**, 26A-33A.
6. X.-P. Yan, R. Kerrich and M. J. Hendry, *Geochim. Cosmochim. Acta*, 2000, **64**, 2637-2648.
7. X. C. Le, M. S. Ma and N. A. Wong, *Anal. Chem.*, 1996, **68**, 4501-4506.
8. B. Welz and M. Sucmanova, *Analyst*, 1993, **118**, 1417-1423.
9. E. H. Larsen and S. Sturup, *J. Anal. Atom. Spectrom.*, 1994, **9**, 1099-1105.
10. M. Mulvihill, A. Tao, K. Benjauthrit, J. Arnold and P. Yang, *Angew. Chem. Int. Ed.*, 2008, **47**, 6456-6460.
11. J. Li, L. Chen, T. Lou and Y. Wang, *ACS Appl. Mater. Inter.*, 2011, **3**, 3936-3941.
12. S. Shen, X.-F. Li, W. R. Cullen, M. Weinfeld and X. C. Le, *Chem. Rev.*, 2013, **113**, 7769-7792.
13. D. Merulla, N. Buffi, S. Beggah, F. Truffer, M. Geiser, P. Renaud and J. R. van der Meer, *Curr. Opin. Biotechnol.*, 2013, **24**, 534-541.
14. S. Sanllorente-Mendez, O. Dominguez-Renedo and M. J. Arcos-Martinez, *Sensors*, 2010, **10**, 2119-2128.
15. X. Fuku, F. Iftikar, E. Hess, E. Iwuoha and P. Baker, *Anal. Chim. Acta*, 2012, **730**, 49-59.
16. X. Dai and R. G. Compton, *Analyst*, 2006, **131**, 516-521.
17. J. R. Kalluri, T. Arbneshi, S. Afrin Khan, A. Neely, P. Candice, B. Varisli, M. Washington, S. McAfee, B. Robinson, S. Banerjee, A. K. Singh, D. Senapati and P. C. Ray, *Angew. Chem., Int. Ed.*, 2009, **48**, 9668-9671.
18. R. Dominguez-Gonzalez, L. Gonzalez Varela and P. Bermejo-Barrera, *Talanta*, 2014, **118**, 262-269.
19. K. Assegid, F. Ahmed, S. Ahamed and A. Hussam, *Anal. Methods*, 2011, **3**, 2921-2928.
20. S. N. Davis and R. J. M. DeWiest, *Hydrogeology*, John Wiley & Sons, Inc., New York, 1966.
21. J. Liu, Z. Cao and Y. Lu, *Chem. Rev.*, 2009, **109**, 1948–1998.
22. H. Zhang, F. Li, B. Dever, X.-F. Li and X. C. Le, *Chem. Rev.*, 2013, **113**, 2812-2841.
23. H. Wang, R. H. Yang, L. Yang and W. H. Tan, *ACS Nano*, 2009, **3**, 2451-2460.
24. D. Li, S. P. Song and C. H. Fan, *Acc. Chem. Res.*, 2010, **43**, 631-641.
25. Y. Du, B. L. Li and E. K. Wang, *Acc. Chem. Res.*, 2013, **46**, 203-213.
26. B. A. Manning, S. E. Fendorf and S. Goldberg, *Environ. Sci. Technol.*, 1998, **32**, 2383-2388.
27. S. Goldberg and C. T. Johnston, *J. Colloid Interf. Sci.*, 2001, **234**, 204-216.
28. F. Frau, D. Addari, D. Atzei, R. Biddau, R. Cidu and A. Rossi, *Water Air Soil Poll.*, 2010, **205**, 25-41.
29. F. Liu, A. De Cristofaro and A. Violante, *Soil Sci.*, 2001, **166**, 197-208.
30. K. P. Raven, A. Jain and R. H. Loeppert, *Environ. Sci. Technol.*, 1998, **32**, 344-349.
31. C. H. Lu, H. H. Yang, C. L. Zhu, X. Chen and G. N. Chen, *Angew. Chem. Int. Ed.*, 2009, **48**, 4785-4787.
32. R. Pautler, E. Y. Kelly, P.-J. J. Huang, J. Cao, B. Liu and J. Liu, *ACS Appl. Mater. Inter.*, 2013, **5**, 6820–6825.
33. X. Zhang, F. Wang, B. Liu, E. Y. Kelly, M. R. Servos and J. Liu, *Langmuir*, 2014, **30**, 839–845.
34. D. J. Maxwell, J. R. Taylor and S. Nie, *J. Am. Chem. Soc.*, 2002, **124**, 9606-9612.
35. H. D. Hill, J. E. Millstone, M. J. Banholzer and C. A. Mirkin, *ACS Nano*, 2009, **3**, 418-424.

36. X. Meng, S. Bang and G. P. Korfiatis, *Water Res.*, 2000, **34**, 1255-1261.
37. S. Dixit and J. G. Hering, *Environ. Sci. Technol.*, 2003, **37**, 4182-4189.
38. M. Kim, H. J. Um, S. Bang, S. H. Lee, S. J. Oh, J. H. Han, K. W. Kim, J. Min and Y. H. Kim, *Environ. Sci. Technol.*, 2009, **43**, 9335-9340.
39. Y. Wu, S. Zhan, H. Xing, L. He, L. Xu and P. Zhou, *Nanoscale*, 2012, **4**, 6841-6849.
40. J. Liu, *Phys. Chem. Chem. Phys.*, 2012, **14**, 10485-10496.

